Application note

Direct in-line quantification of titer in clarified harvest using Raman spectroscopy

Authors

Nimesh Khadka[1], Ph.D.
Lin Zhang[1], Ph.D.
Michelle Nolasco[2]

[1]Analytical Instrument Group, ThermoFisher Scientific, Tewksbury, Massachusetts USA

[2]BioProduction Group, ThermoFisher Scientific, St. Louis, Missouri USA

Thermo Scientific MarqMetrix All-In-One Process Raman Analyzer, Thermo Scientific MarqMetrix Performance BallProbe Sampling Optic.

Industry/Application:
Biopharma PAT / Downstream

Products used:
Thermo Scientific™ MarqMetrix™ All-In-One Process Raman Analyzer, Thermo Scientific™ MarqMetrix™ Performance BallProbe™ Sampling Optic

Goals:
Eliminating offline analytics with real time titer quantification using process Raman in a clarified harvest

Key Analytes:
Titer; monoclonal antibody; clarified harvest

Key Benefits:

- Raman analysis streamlines downstream biopharma processes with cost and time benefits by eliminating the need for offline chromatographic analysis when calculating loading volume.
- This methodology paves a path toward automation and continuous manufacturing by coupling upstream and downstream processes

Introduction

Monoclonal antibodies (mAbs) are manufactured in two stages: upstream and downstream processes, as shown in Figure 1. In the upstream process, cells are cultured to produce mAbs. These mAbs are then purified in the downstream process through a series of chromatography and filtration operations. Before chromatographic purification, cells and debris are removed by centrifugation and/or depth filtration in a process called clarification. The resulting supernatant after clarification, known as clarified harvest, contains the desired product (mAb), along with soluble metabolites and waste products. The clarified harvest is then subjected to further downstream processing to isolate and purify the target mAb.

Knowing the concentration of the mAb (titer) in the clarified harvest before loading onto an affinity (capture) chromatography column (e.g., protein A) is essential for several reasons. It allows for the determination of loading volumes, ensuring the column is loaded with the right amount of clarified harvest to maximize the resin binding capacity. Overloading the column can lead to incomplete binding of the mAb, product loss, and, thereby, reduced purification efficiency. Since Raman spectroscopy provides real-time measurements, it facilitates continuous manufacturing and automation from the upstream bioreactor run to the clarification step to downstream purification, eliminating the need for conventional laboratory analytics and significantly reducing the time otherwise required for HPLC to measure titer concentration. In this study, we demonstrate the capability of process Raman to directly quantify the titer in the clarified harvest without any need of sample preparation.

Experimental details

Data collection

Calibration samples with known mAb concentration were obtained from multiple bioreactor conditions. The titer in clarified samples ranged between 0 and 9 g/L. The samples were prepared by mixing titer-free clarified harvest (filtrate collected during protein A affinity column) with purified mAb to create different concentration of training samples using the design of experiment (DoE) approach based on the algorithm of Uniform Design (UD).[1] Each sample was scanned with a Thermo Scientific™ MarqMetrix™ Performance BallProbe™ Sampling Optic integrated with the Thermo Scientific™ MarqMetrix™ All-In-One Process Raman Analyzer. The acquisition parameters were set to a power of 450 mW, an integration time of 5000 ms, and an average of 10 spectra, resulting in a spectrum every 2 minute.

Chemometric model development

The spectral regions 775 to 1920 cm^{-1} were selected to develop the Partial Least Square (PLS) model for titer quantification (Figure 2A). Baseline was removed from each spectrum using automatic Whittaker filter with the parameters for asymmetry and lambda set to 0.001 and 1000 respectively. Each spectrum was then normalized using the L1 norm calculated for the region 1590 to 1655 cm^{-1}. To improve the model performance, all spectra were derivatized using a Savitzky-Golay filter (1st derivative; order = 2; window width =9) followed by mean centering.

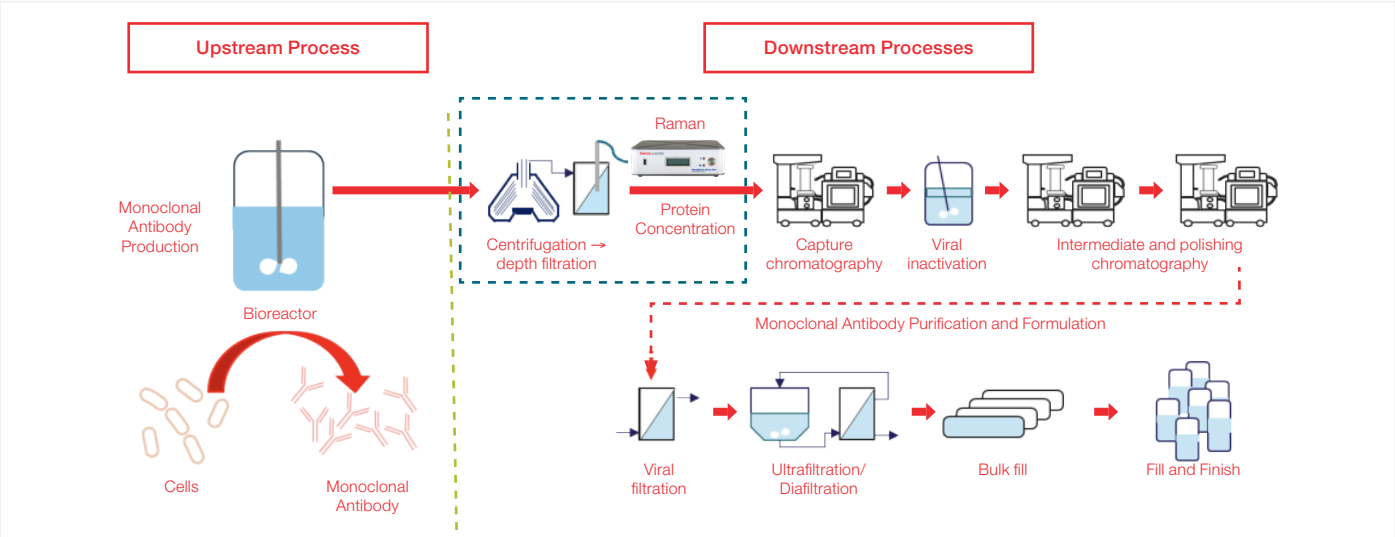

Figure 1. The workflow for the manufacturing of monoclonal antibodies. Also highlighted is the clarification step by the blue dotted box where in-line process Raman was used for real time titer concentration measurement.

The number of latent variables (LVs) for the PLS model was selected using leave-one-out cross-validation (LOOCV). During this process, each unique concentration block was left out from model training and used in prediction exactly once, and all replicates for a given concentration were treated as a single block to prevent data leakage. The optimal number of LVs was determined by minimizing the root mean square error of calibration and cross-validation while maintaining their ratios close to 1.

The developed PLS model for the clarified harvest titer was evaluated using a validation set prepared with the DoE approach and by applying it to Raman data acquired from samples collected from different clarified harvests.

All data management, cosmic ray removal, averaging, and timestamp alignment were performed in Python. All chemometric works were performed using software package SOLO 9.3.1 (2024). Eigenvector Research. Inc. Manson, WA USA 98831.

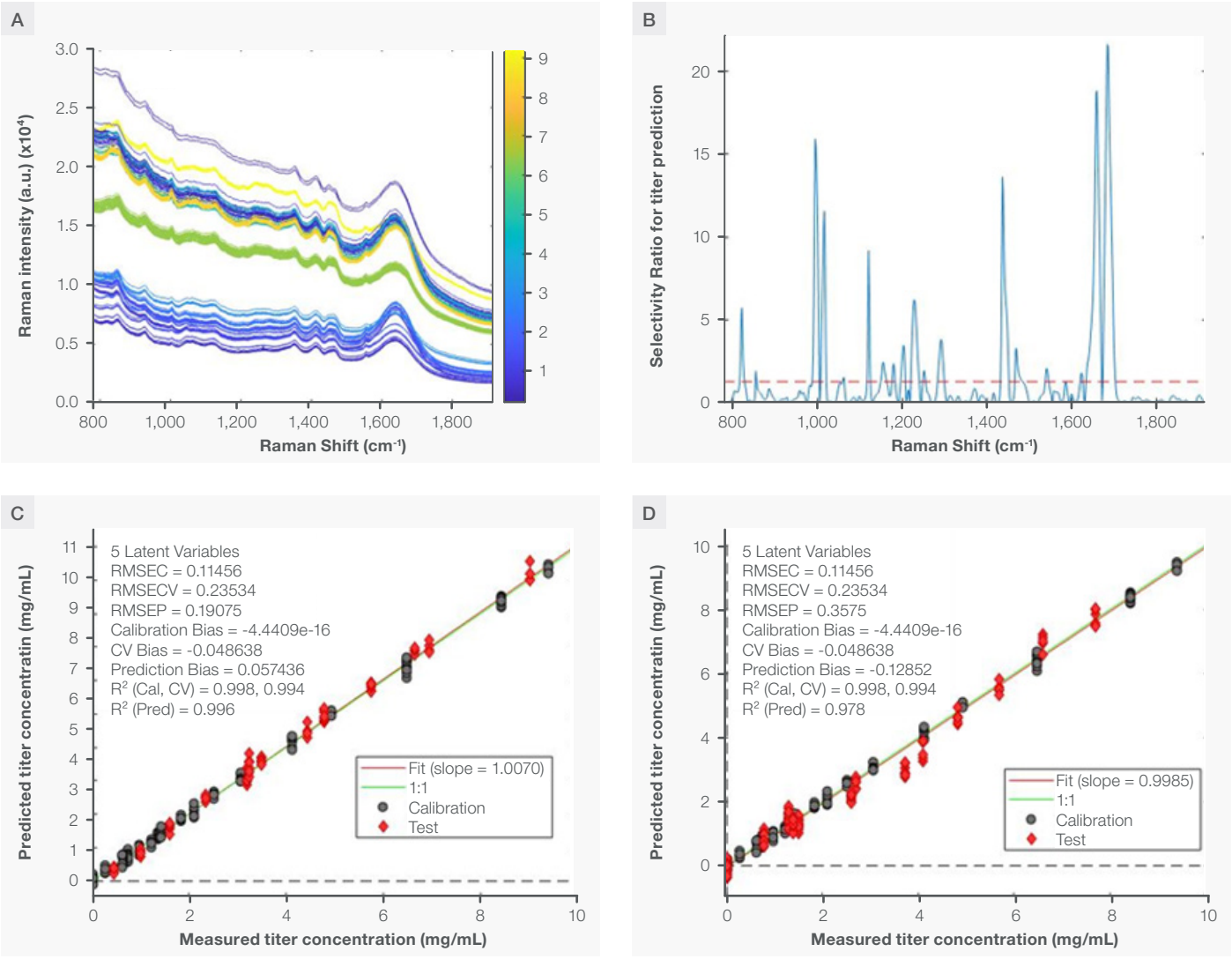

Figure 2. The spectral region used to develop the titer PLS model is shown in plot A. The selectivity ratio (SR) plot is shown in B and indicates the Amide I spectral region (1650 to 1700 cm^{-1}) has strong influence in the model performance and specificity. Plot C and D show the predictive performance of the model for the DoE samples and different batches of clarified harvest, respectively. The gray filled circle are training data and red diamond are test data.

Results and discussion

The PLS model was developed using five latent variables (LVs). The root mean square error of calibration (RMSEC) and cross-validation (RMSECV) were 0.114 mg/mL and 0.235 mg/mL, respectively. The specificity of the model was evaluated by calculating the selectivity ratio (SR), as shown in Figure 2B. The SR is the ratio of the explained variance to residual variance for each Raman shift.[2] A higher SR for a given Raman shift indicates its greater importance for the model, forming the basis for model specificity. The Raman shifts between 1650 to 1700 cm^{-1} for the developed PLS model had high SR. This region, known as the Amide I region, primarily includes the Raman signature associated with the symmetrical stretching of the carbonyl group of the amide (peptide) linkage.[3] Depending on the location of the carbonyl group in different secondary structures, they experience different electronic environments and thus have different energies associated with the symmetrical stretching of the carbonyl group. The Amide I region provides molecular information on the secondary structure of the protein, where its total area is proportional to the total amount of carbonyl functional groups present in the protein, and its features or peak positions depend on the presence of different secondary structures. The titer (mAbs) is a globular protein, and its secondary structure is dominated by β-sheet structure. As shown in Figure 2B, the SR ratio at ~ 1670 cm^{-1} is most prominent; this can be assigned to the symmetrical stretching of carbonyl group in the β-sheet structure. Thus, Amide I region contributes to the specificity for titer quantification in the clarified harvest. Similarly, the CH deformation (~1440 cm^{-1}), Amide III region (~ 1230 cm^{-1}; symmetric stretching C-N (ν(C-N)), N-H bending (δ(N-H)), symmetric C-C stretch (~1130 cm^{-1}), phenylalanine ring breathing mode (~1005 cm^{-1}), and tyrosine doublet (~830 and 850 cm^{-1}) due to Fermi resonance between the in-plane breathing mode of the phenol ring and an overtone of out-of-plane deformation mode are other Raman features of titer that are influential in the model.[4] All these features collectively provide specificity for the model to quantify titer against the matrix of the host cell proteins (HCPs), metabolites, and other waste products. The model performance when applied to the independent validation set is shown in Figures 2C and 2D.

Initially, the model was applied to the validation set samples prepared using the Uniform Design. The root means square error of prediction (RMSEP) was 0.19 mg/mL across the concentration range of 0 to 9 mg/mL. Similarly, when the model was applied to different batches of clarified harvest samples, the average RMSEP was 0.36 mg/mL. The offline analysis on the clarified harvest samples revealed that different batches of clarified harvest had varying matrices, including differences in the concentration and composition of HCPs, metabolites, and other molecules. After preprocessing, overlaying, and color-coding the training and clarified harvest datasets with titer concentration, a clear correlation was observed between Raman intensity and concentration in the spectral regions around 1670 cm^{-1}, 1440 cm^{-1}, 1005 cm^{-1}, 830 cm^{-1}, and 850 cm^{-1} as shown in Figure 3. However, other spectral regions exhibited strong interference from the Raman signatures of the matrices, likely from Raman signals from the HCPs, resulting in a lack of correlation between Raman intensity and titer concentration in these spectral regions. These findings validated the model's specificity, as shown in the specificity plot (Figure 2B), and insight into the value of multivariate chemometrics in extracting useful information from complex spectra. Since HCPs vary between batches, it is recommended to augment the titer model with multiple batches of clarified harvest process data. This approach could further optimize the model by capturing process variations, thereby improving performance and lowering the RMSEP.

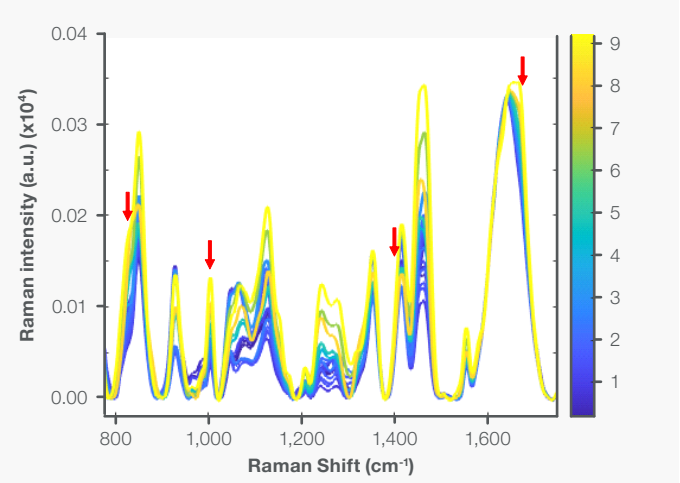

Figure 3. Spectral overlay of the preprocessed training and test datasets (different batches of clarified harvest). The spectra are color-coded by titer concentrations, as indicated by the vertical bar. The red arrow points to the spectral regions that visually correlate with titer concentrations. Uncorrelated spectral regions are mainly due to Raman signals from host cell proteins.

Conclusion

In this study, we demonstrated real-time quantification of titer in the complex matrix of clarified harvest without any sample preparation. The results indicate that by implementing in-line process Raman in the workflow, users can eliminate the need for conventional offline HPLC analysis to quantify titer in clarified harvest. Thus, users can directly proceed to the downstream purification step by reliably calculating the loading volumes for purification columns. This result not only demonstrates the capability of Raman spectroscopy for complex mixture analysis by leveraging unique molecular Raman signatures, but also provides a practical solution with time and cost benefits to the user. We and others have previously demonstrated Raman as a reliable tool for monitoring and feedback control of upstream and downstream processes.[5–9] The results shown here directly bridge our previous works by coupling upstream with downstream processes and establish process Raman as a single sensor with wide applications for biomanufacturing, as well as achieving automated continuous manufacturing.

References

1. Zhang, L.; Liang, Y.-Z.; Jiang, J.-H.; Yu, R.-Q.; Fang, K.-T. Uniform Design Applied to Nonlinear Multivariate Calibration by ANN. *Anal. Chim. Acta* **1998**, *370* (1), 65–77. https://doi.org/10.1016/S0003-2670(98)00256-6.
2. Kvalheim, O. M. Variable Importance: Comparison of Selectivity Ratio and Significance Multivariate Correlation for Interpretation of Latent-Variable Regression Models. *J. Chemom.* **2020**, *34* (4), e3211. https://doi.org/10.1002/cem.3211.
3. Peters, J.; Park, E.; Kalyanaraman, R.; Luczak, A.; Ganesh, V. Protein Secondary Structure Determination Using Drop Coat Deposition Confocal Raman Spectroscopy. **2016**, *31*, 31–39.
4. Dolui, S.; Mondal, A.; Roy, A.; Pal, U.; Das, S.; Saha, A.; Maiti, N. C. Order, Disorder, and Reorder State of Lysozyme: Aggregation Mechanism by Raman Spectroscopy. *J. Phys. Chem. B* **2020**, *124* (1), 50–60. https://doi.org/10.1021/acs.jpcb.9b09139.
5. Abu-Absi, N. R.; Kenty, B. M.; Cuellar, M. E.; Borys, M. C.; Sakhamuri, S.; Strachan, D. J.; Hausladen, M. C.; Li, Z. J. Real Time Monitoring of Multiple Parameters in Mammalian Cell Culture Bioreactors Using an In-Line Raman Spectroscopy Probe. *Biotechnol. Bioeng.* **2011**, *108* (5), 1215–1221. https://doi.org/10.1002/bit.23023.
6. Villa, J.; Zustiak, M.; Kuntz, D.; Zhang, L.; Woods, S.; Scientific, F. Real Time Metabolite Monitoring Using the MarqMetrix All-In-One Process Raman Analyzer and the 500L HyPerforma Dynadrive Single-Use Bioreactor (S.U.B.).
7. Villa, J.; Zustiak, M.; Kuntz, D.; Zhang, L.; Khadka, N.; Broadbelt, K.; Woods, S. Use of Lykos and TruBio Software Programs for Automated Feedback Control to Monitor and Maintain Glucose Concentrations in Real Time.
8. Nolasco, M.; Pleitt, K.; Khadka, N. Using a Process Raman Analyzer as an In-Line Tool for Accurate Protein Quantification in Downstream Processes.
9. Nolasco, M.; Pleitt, K.; Khadka, N. Raman-Based Accurate Protein Quantification in a Matrix That Interferes with UV-Vis Measurement.

Learn more at **thermofisher.com**